

A Small Molecule Agonist of an Integrin, $\alpha_L\beta_2$ *[§]

Received for publication, July 19, 2006 Published, JBC Papers in Press, October 5, 2006, DOI 10.1074/jbc.M606888200

Wei Yang^{‡§1}, Christopher V. Carman^{‡§1}, Minsoo Kim^{‡§1,2}, Azucena Salas^{‡§1,3}, Motomu Shimaoka^{‡¶1},
and Timothy A. Springer^{‡§4}

From the [‡]CBR Institute for Biomedical Research, Departments of [§]Pathology and [¶]Anesthesia, Harvard Medical School, Boston, Massachusetts 02115

The binding of integrin $\alpha_L\beta_2$ to its ligand intercellular adhesion molecule-1 is required for immune responses and leukocyte trafficking. Small molecule antagonists of $\alpha_L\beta_2$ are under intense investigation as potential anti-inflammatory drugs. We describe for the first time a small molecule integrin agonist. A previously described α/β I allosteric inhibitor, compound 4, functions as an agonist of $\alpha_L\beta_2$ in Ca^{2+} and Mg^{2+} and as an antagonist in Mn^{2+} . We have characterized the mechanism of activation and its competitive and noncompetitive inhibition by different compounds. Although it stimulates ligand binding, compound 4 nonetheless inhibits lymphocyte transendothelial migration. Agonism by compound 4 results in accumulation of $\alpha_L\beta_2$ in the uropod, extreme uropod elongation, and defective de-adhesion. Small molecule integrin agonists open up novel therapeutic possibilities.

Integrins are a large family of α/β heterodimeric cell surface receptors that mediate cell-cell and cell-extracellular matrix adhesion and transduce signals bidirectionally across the plasma membrane. Integrin $\alpha_L\beta_2$ (lymphocyte function associated antigen-1 (LFA-1))⁵ belongs to the β_2 integrin subfamily and is constitutively expressed on all leukocytes. $\alpha_L\beta_2$ remains in a low affinity state in resting lymphocytes and undergoes dramatic conformational change during lymphocyte activation, which greatly increases its binding affinity for its ligands intercellular adhesion molecule -1, -2, and -3 (ICAM-1, -2, and

-3). Regulation of $\alpha_L\beta_2$ activation is pivotal for controlling leukocyte trafficking and immune responses in health and diseases (1–3).

$\alpha_L\beta_2$ is an important pharmaceutical target for treating autoimmune and inflammatory diseases (4–8). A humanized antibody to $\alpha_L\beta_2$ that blocks its binding to the ligand ICAM-1 has been approved by the FDA for treatment of psoriasis, a T cell-mediated autoimmune disease of the skin (9, 10). Furthermore, small molecule antagonists of $\alpha_L\beta_2$ have been discovered and are in development (11–17).

$\alpha_L\beta_2$ contains two von Willebrand factor-type A domains, the inserted (I) domains in the α_L and the β_2 subunits (18–20). Both α_L I and β_2 I domains have a Rossman fold (*i.e.* a central β -sheet surrounded by α -helices) with a metal ion-dependent adhesion site (MIDAS) formed by β - α loops at the “top” face of the domain (20–23). In ligand binding the Mg^{2+} ion in the MIDAS of the α_L I domain coordinates directly to a Glu residue that is in the center of the ligand binding sites in domain 1 of ICAM-1 and ICAM-3 (20, 24). The affinity of the α_L I domain for ICAMs is regulated by downward axial displacement of its C-terminal $\alpha 7$ helix, which is conformationally linked to reshaping of MIDAS loops and increases affinity for ligand by up to 10,000-fold (25, 26). During activation, the β I domain undergoes similar $\alpha 7$ helix downward axial movement, which is induced by the swing out of the hybrid domain (27–30).⁶ Previous data suggested that when activated, the β_2 I domain binds (through the Mg^{2+} in its MIDAS) to the Glu residue (Glu-310) in the C-terminal linker of the α_L I domain, exerts a downward pull on its $\alpha 7$ helix, and thereby activates the α_L I domain (Fig. 1A) (32, 33).

Two distinct classes of small molecule antagonists of $\alpha_L\beta_2$ have been developed as anti-inflammatory agents. One group of antagonists binds the hydrophobic pocket underneath the $\alpha 7$ helix of the α_L I domain (*e.g.* LFA703 or BIRT377), blocks the downward axial movement of the $\alpha 7$ helix, and inhibits ligand binding of $\alpha_L\beta_2$ allosterically by stabilizing the α_L I domain in the low affinity conformation (11–14, 34). These antagonists are called α I allosteric inhibitors. The other group of antagonists appears to bind to the β_2 I domain MIDAS near a key regulatory interface with the α_L I domain, blocking communication of conformational change to the α_L I domain while at the same time activating conformational rearrangements elsewhere in integrins (35–37). These antagonists, such as compounds 3 and 4 from Genentech and XVA143 from Hoffmann-La Roche, are called α/β I allosteric inhibitors (Fig. 1B). In this report, however, we describe that compound 4, previ-

* This work was supported by National Institutes of Health Grants CA31798 (to T. A. S.) and AI63421 (to M. S.) and a grant from the Arthritis Foundation (to C. V. C.). The costs of publication of this article were defrayed in part by the payment of page charges. This article must therefore be hereby marked “advertisement” in accordance with 18 U.S.C. Section 1734 solely to indicate this fact.

[§] The on-line version of this article (available at <http://www.jbc.org>) contains supplemental Videos 1 and 2.

¹ These authors contributed equally to this work.

² Current address: Division of Surgical Research, Rhode Island Hospital, Brown University School of Medicine, 593 Eddy Street, Middlehouse 207, Providence, RI 02903.

³ Current address: Instituto de Investigaciones Biomédicas de Barcelona-CSIC, Roselló 161, 7^a planta, 08036 Barcelona, Spain.

⁴ To whom correspondence should be addressed: The CBR Institute for Biomedical Research, Dept. of Pathology, Harvard Medical School, 200 Longwood Ave., Boston, MA 02115. Tel.: 617-278-3200; Fax: 617-278-3232; E-mail: springeroffice@cbr.med.harvard.edu.

⁵ The abbreviations used are: LFA-1, lymphocyte function associated antigen-1; ICAM, intercellular adhesion molecule; MIDAS, metal ion-dependent adhesion site; mAb, monoclonal antibody; PBMC, peripheral blood mononuclear cell; HUVEC, human umbilical vein endothelial cell; FRET, fluorescence resonance energy transfer; TNF, tumor necrosis factor; mCFP, monomeric cyan fluorescent protein; mYFP, monomeric yellow fluorescent protein.

⁶ Nishida, N., Xie, C., Shimaoka, M., Cheng, Y., Walz, T., and Springer, T. A., (2006) *Immunity* **25**, 583–594.

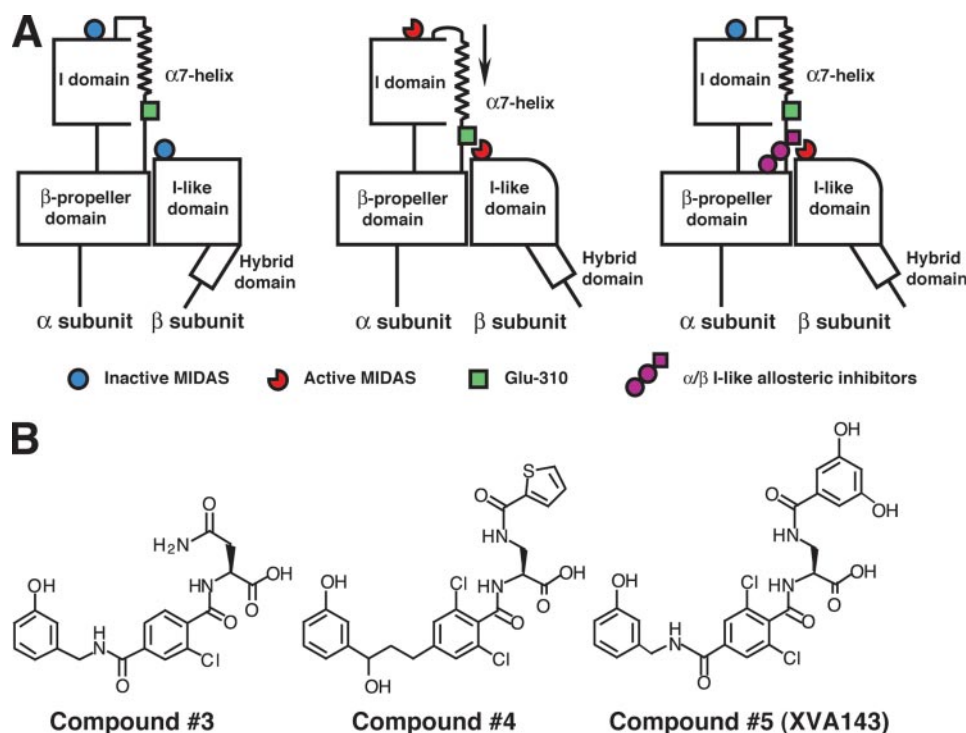


FIGURE 1. Mechanisms of inhibition and chemical structures of α/β I allosteric antagonists. *A*, mechanisms of inhibition and impact on integrin conformation of α/β I allosteric antagonists. α/β I allosteric inhibitors bind to the β_2 I domain MIDAS near a key regulatory interface with the α_L I domain and block communication of conformational change to the I domain while at the same time activating conformational rearrangements elsewhere in integrins, including swing-out of the hybrid domain. *B*, chemical structures of α/β I allosteric antagonists.

ously regarded as an α/β I allosteric inhibitor based on studies in Mn^{2+} , actually activates $\alpha_L\beta_2$ under physiological conditions in Ca^{2+} , and Mg^{2+} and inhibits integrin-dependent functions by perturbing de-adhesion.

EXPERIMENTAL PROCEDURES

Antibodies and Small Molecule Inhibitors—mAbs to human α_L and β_2 are as described (34). m24 (38) and KIM127 (39) were kind gifts of N. Hogg (London Research Institute) and M. Robinson (Celltech, Slough, UK), respectively. Compound 5 (XVA143) was synthesized according to example 345 of the patent (35) and was also obtained from P. Gillespie (Hoffmann-La Roche). Compounds 3 and 4 were obtained from Genentech (South San Francisco, CA) through the research reagents program. LFA703 (11, 12) was provided by Novartis Pharma AG (Basel, Switzerland), and BIRT377 was from T. Kelly (Boehringer Ingelheim Pharmaceuticals Inc, Ridgeway, CT).

Cell Isolation and Culture—K562 transfectants expressing wild-type and mutant $\alpha_L\beta_2$ were described (40). Preparation of human peripheral blood mononuclear cells (PBMCs) and interleukin-2-cultured primary lymphocytes was previously described (41). Primary human umbilical vein endothelial cells (HUVECs) were from Cambrex (Walkersville, MD) and cultured as confluent monolayers on fibronectin (10 μ g/ml) coated on glass coverslips or ΔT live-cell imaging chambers (Bioprotech, Butler, PA) in EGM-2 complete media (Cambrex, Walkersville, MD).

Binding of Soluble ICAM-1—Binding of soluble ICAM-1-IgA Fc fusion protein complexed with affinity-purified, fluorescein isothiocyanate-conjugated anti-human IgA was measured by flow cytometry (37).

Cell Adhesion to Immobilized ICAM-1—Binding of fluorescently labeled transfectants to immobilized ICAM-1 was as described (40). Briefly, ICAM-1-IgG Fc fusion protein at 10 μ g/ml was immobilized on microtiter plates previously coated with 20 μ g/ml protein A and blocked with 2% human serum albumin. Binding of transfectants to immobilized ICAM-1 was determined in Hepes, NaCl, glucose, bovine serum albumin (BSA; 20 mM Hepes, pH 7.5, 140 mM NaCl, 2 mg/ml glucose, 1% BSA) supplemented with divalent cations and compounds as indicated. After incubation at 37 $^{\circ}C$ for 30 min, unbound cells were washed off, and bound cells were quantitated (40).

Flow Chamber Assay—Binding and detachment in shear flow of $\alpha_L\beta_2$ transfectants on immobilized

ICAM-1 substrates was done in a parallel plate flow chamber as described (42).

Fluorescence Resonance Energy Transfer (FRET) Assay—FRET assay using α_L -monomeric cyan fluorescent protein (mCFP)/ β_2 -monomeric yellow fluorescent protein (mYFP) K562 stable transfectants was as described (43).

Cell Migration Assays—Lymphocyte transendothelial migration assays were as described (41). Briefly, before each experiment confluent HUVEC monolayers were activated for 12 h with TNF- α (100 ng/ml). HUVECs were then washed 3 times in buffer A (Hanks' balanced salt solution supplemented with 20 mM Hepes, pH 7.2, and 1% human serum albumin). Interleukin 2-cultured primary human lymphocytes were pelleted, resuspended at 100,000 cells/ml in 500 μ l of buffer A containing compound 4 (1 μ M), compound 5 (1 μ M), BIRT377 (20 μ M), or CBR LFA-1/2 Fab (20 μ g/ml) and then added to HUVECs and incubated at 37 $^{\circ}C$ for 10 or 60 min. Samples were fixed in 3.7% formaldehyde in phosphate-buffered saline for 5 min and stained for leukocyte α_L integrin (TS2/4 mAb conjugated to Cy3), endothelial cell ICAM-1 (IC1/11 mAb conjugated to Alexa488), and F-actin (phalloidin-Alexa647; Molecular Probes) as described (41). Imaging was conducted using Bio-Rad Radiance 2000 Laser-scanning confocal microscope system. For each condition complete Z-stacks (0.5 μ m thickness) were obtained in each of ten randomly selected fields. Using LaserSharp 2000 software (Bio-Rad) Z-stacks were analyzed (based on previously described criteria (41)) to determine the

Small Molecule Agonist of an Integrin, $\alpha_L\beta_2$

number of cells in the process of, or having completed diapedesis.

Morphological analysis of the apically adherent lymphocyte population was based both on the overall cell shape and the distribution of actin and $\alpha_L\beta_2$. Cells exhibiting generally even actin and $\alpha_L\beta_2$ distributions and either spherical or symmetrically spread shapes were designated as “round” or “spread”, respectively. Cells exhibiting polarized shapes with an actin-enriched leading edge and roughly even distribution of LFA-1 were designated “polarized”. Cells that exhibited both extended uropods and sequestration of the majority of the cellular LFA-1 to the uropod were designated as “X-polarized” (*i.e.* extremely polarized).

For live-cell experiments confluent TNF- α -activated HUVEC monolayers were prepared on Biopetechs ΔT imaging chambers, rinsed three times with buffer A, and maintained at 37 °C. Lymphocytes (100,000) were added to the chambers, and differential interference contrast images were acquired (using a Zeiss Axiovert S200 epifluorescence microscope (Germany) equipped with a 63 \times oil objective coupled to a Hamamatsu Orca CCD (Japan)) at 5-s intervals over a course of 30 min. Cell migration was analyzed by manually tracing the outline of each cell in selected frames (*i.e.* at 180-s intervals) for each time course. Lines connecting the centroid of each cell outline (automatically calculated by OpenLab software) were generated to represent the migration path or “track” followed by each lymphocyte. The total length of the cell tracks was divided by the total time interval during which the track was recorded to calculate average migration velocity. The linear distance between the beginning and endpoint of each track was measured to determine the overall displacement of each cell. Measurement of cell lateral migration parameters was restricted to lymphocytes during their migration over the apical surface of the endothelium and discontinued upon diapedesis across the endothelial monolayer to the subendothelial space. The percentage of diapedesis was obtained by dividing the number of cells that initiated diapedesis by the total number of migrating cells.

To analyze the qualitative details of migration behavior, representative cells were traced at 50-s intervals. The distance separating the centroid of the cell in the initial frame and the centroid of the cell at each subsequent interval was plotted against the cumulative time elapsed.

Online Supplemental Material—Supplemental Videos 1 and 2 are representative videos of lymphocyte migration in the absence (Video 1) and presence (Video 2) of compound 4 as described in Figs. 7, C and D, respectively.

RESULTS

Compound 4 Activates $\alpha_L\beta_2$ in Physiologic Cations ($\text{Ca}^{2+}/\text{Mg}^{2+}$) but Inhibits in Mn^{2+}

K562 cells expressing $\alpha_L\beta_2$ showed little binding to soluble multimeric ICAM-1 in $\text{Ca}^{2+}/\text{Mg}^{2+}$ (Fig. 2A), whereas binding was greatly increased by Mn^{2+} (Fig. 2B) or the activating mAb CBR LFA-1/2 (Fig. 2C). In Mn^{2+} , compounds 3–5 potently inhibited soluble, multimeric ICAM-1 binding by $\alpha_L\beta_2$ (Fig. 2B), consistent with previous observations (17, 37). However, in physiologic cations (*i.e.* 1 mM Ca^{2+} and 1 mM Mg^{2+}) we found,

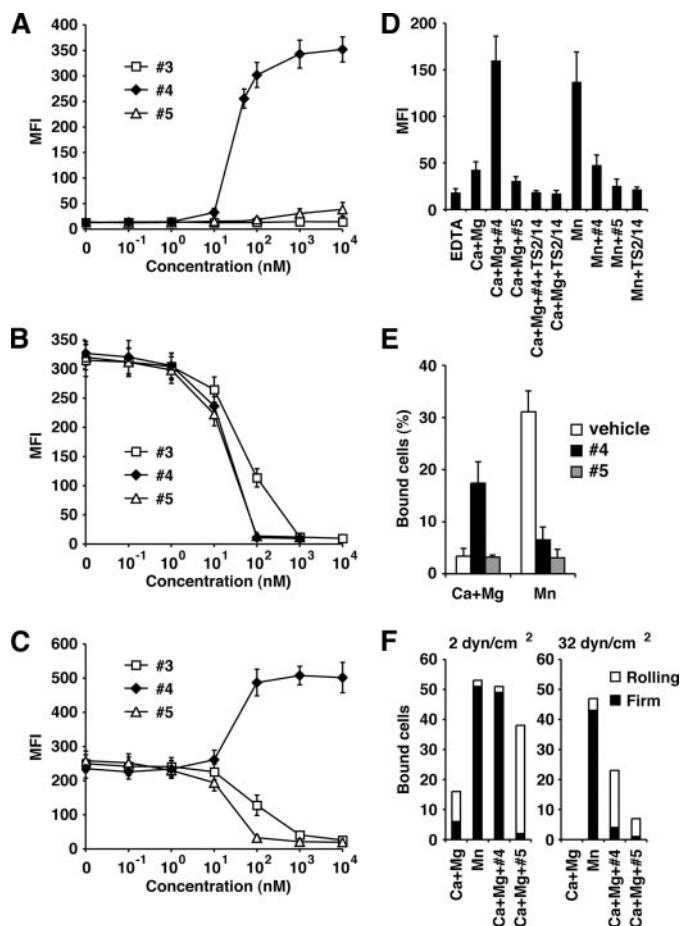


FIGURE 2. Compound 4 inhibits $\alpha_L\beta_2$ in Mn^{2+} but activates $\alpha_L\beta_2$ in Ca^{2+} and Mg^{2+} . A–C, soluble multimeric ICAM-1 binding by K562 stable transfectants expressing wild-type $\alpha_L\beta_2$. Cells were incubated with compounds in Heps, NaCl, glucose, bovine serum albumin supplemented with 1 mM CaCl_2 and 1 mM MgCl_2 (A), 2 mM MnCl_2 (B), or 1 mM CaCl_2 , 1 mM MgCl_2 , and 10 $\mu\text{g}/\text{ml}$ CBR LFA-1/2 (C) for 30 min at room temperature. Then fluorescein isothiocyanate-labeled multimeric ICAM-1 was added and incubated with cells for another 30 min at room temperature. The binding was detected by flow cytometry and is expressed as mean fluorescence intensity (MFI). D, soluble multimeric ICAM-1 binding by human PBMCs was assayed as in A–C with cations, compounds (1 μM), and TS2/14 mAb (10 $\mu\text{g}/\text{ml}$) as indicated. E, static adhesion of $\alpha_L\beta_2$ -expressing K562 cells to immobilized ICAM-1 was as described in “Experimental Procedures” with cations and compounds (1 μM) as indicated. F, adhesion in shear flow of $\alpha_L\beta_2$ -expressing K562 cells to immobilized ICAM-1. K562 cells expressing wild-type $\alpha_L\beta_2$ were incubated in media containing different divalent cations and compounds (1 μM) as above. Cells were allowed to accumulate on an ICAM-1-Fc-coated substrate at 0.3 dyn/cm^2 in the flow chamber for 30 s before increasing the flow rate every 10 s in about 2-fold increments to the indicated wall shear stresses. Bars show the total number of adherent cells, including cells that were rolling (white) or firmly adherent (black).

unexpectedly, that compound 4 greatly increased ligand binding, whereas compounds 3 and 5 had no effect (Fig. 2A). Furthermore, activation of $\alpha_L\beta_2$ binding to ICAM-1 in $\text{Ca}^{2+}/\text{Mg}^{2+}$ by CBR LFA-1/2 mAb was further increased by compound 4 but inhibited by compounds 3 and 5 (Fig. 2C).

Next we assessed the effects of these compounds on physiologic leukocytes (*i.e.* primary human PBMCs). The PBMCs showed weak binding to soluble multimeric ICAM-1 in $\text{Ca}^{2+}/\text{Mg}^{2+}$ alone and significant binding in Mn^{2+} alone (Fig. 2D). Consistent with our observations with K562 transfectants (Fig. 2, A–C), compound 4 strongly increased binding of soluble ICAM-1 to PBMCs in $\text{Ca}^{2+}/\text{Mg}^{2+}$ but inhibited Mn^{2+} -in-

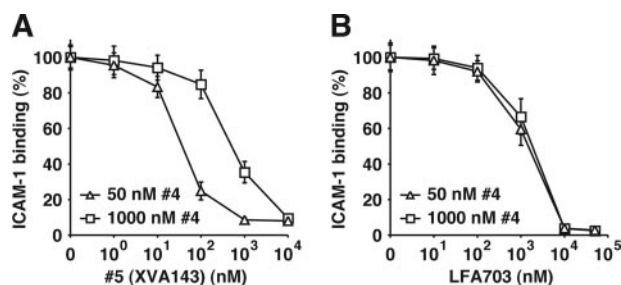


FIGURE 3. Inhibition of agonism by compound 4 with compound 5 and LFA703. Soluble, multimeric ICAM-1 binding by $\alpha_L\beta_2$ -expressing K562 cells was determined as described in Fig. 2A in 1 mM CaCl_2 , 1 mM MgCl_2 after co-incubation with the indicated concentrations of compound 4 and compound 5 (A) or LFA703 (B).

duced binding (Fig. 2D). Both compound 4- and Mn^{2+} -induced ICAM-1 binding was $\alpha_L\beta_2$ -dependent, as such binding was completely inhibited by the α_L I domain-specific blocking antibody TS2/14 (Fig. 2D).

The activating effect of compound 4 was confirmed and further analyzed using static cell adhesion and flow chamber assays. In the static cell adhesion assay, K562 cells expressing $\alpha_L\beta_2$ were allowed to adhere to immobilized ICAM-1, and the unbound cells were removed with an automatic plate washer. In the presence of $\text{Ca}^{2+}/\text{Mg}^{2+}$ alone very little cell adhesion was observed, whereas in the presence of Mn^{2+} alone adhesion was greatly enhanced (Fig. 2E). The addition of either compound 4 or 5 abolished Mn^{2+} -induced adhesion. In contrast, in $\text{Ca}^{2+}/\text{Mg}^{2+}$ compound 4, but not compound 5, greatly increased cell adhesion (Fig. 2E). In a flow chamber assay, K562 cells expressing $\alpha_L\beta_2$ showed weak rolling and firm adhesion to immobilized ICAM-1 in $\text{Ca}^{2+}/\text{Mg}^{2+}$ (Fig. 2F). As demonstrated previously, the addition of compound 5 in $\text{Ca}^{2+}/\text{Mg}^{2+}$ significantly increased rolling adhesion, and Mn^{2+} increased firm adhesion (42). At a shear stress of 2 dyn/cm², compound 4 in $\text{Ca}^{2+}/\text{Mg}^{2+}$ induced firm adhesion to a similar extent as observed with Mn^{2+} alone. Under a high shear regime of 32 dyn/cm² compound 4 still promoted significant adhesion (Fig. 2F). However, the total number of rolling and firmly adherent cells was reduced by about half, whereas the amount of adhesion in Mn^{2+} alone remained essentially unchanged. Thus, $\alpha_L\beta_2$ adhesiveness induced by compound 4 is less shear-resistant than adhesiveness induced by Mn^{2+} .

The Activating Effect of Compound 4 Is Inhibited by Compound 5 Competitively—Compound 4 and compound 5 have homologous structures, and our previous findings suggested that both compounds bind to the MIDAS of the β_2 I domain (37). However, in $\text{Ca}^{2+}/\text{Mg}^{2+}$, compound 4 was activating, whereas compound 5 was inhibitory to wild type $\alpha_L\beta_2$ (Fig. 2). Therefore, we studied whether ICAM-1 binding to $\alpha_L\beta_2$ in $\text{Ca}^{2+}/\text{Mg}^{2+}$ stimulated by compound 4 could be competitively inhibited by compound 5. We found that $\alpha_L\beta_2$ activation by 50 nM compound 4 was reversed by compound 5 in a dose-dependent manner (Fig. 3A). Importantly, the inhibitory dose-response curve of compound 5 was shifted significantly to the right in the presence of a higher concentration (1 μM) of compound 4 (Fig. 3A). Such concentration dependence demonstrates a competitive mode of inhibition. Binding to ICAM-1 stimulated by compound 4 was also inhibited by an α I allosteric

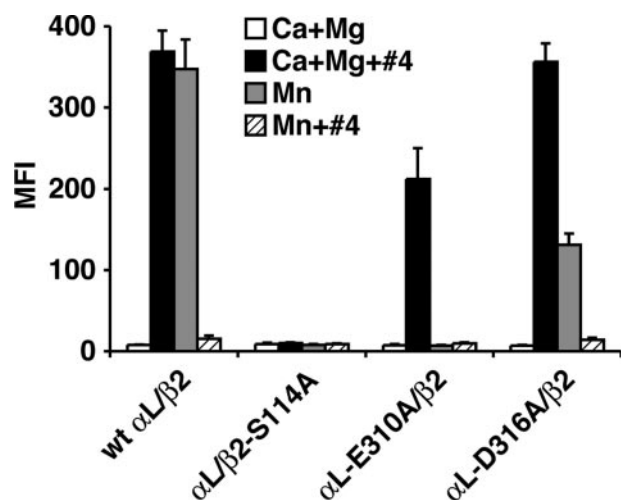


FIGURE 4. Compound 4 and Mn^{2+} activate $\alpha_L\beta_2$ by different mechanisms. Soluble ICAM-1 binding by K562 transfectants expressing wild-type or mutant $\alpha_L\beta_2$ was as described in Fig. 2A in the presence of cations and compounds (1 μM) as indicated. MFI, mean fluorescence intensity.

inhibitor, LFA703, that binds the hydrophobic pocket underneath the α_7 helix of the α_L I domain (Fig. 3B). However, the inhibitory dose-response curve of LFA703 was identical with 50 and 1000 nM compound 4, demonstrating non-competitive inhibition.

Compound 4 and Mn^{2+} Activate $\alpha_L\beta_2$ by Different Mechanisms—The interaction between the β_2 MIDAS and an acidic residue in the C-terminal linker of α I domains, e.g. Glu-310 in α_L , is indispensable for Mn^{2+} -induced activation of β_2 integrins (32, 33, 44). Mutation of either the metal-coordinating MIDAS residue Ser-114 in the β_2 I domain or Glu-310 in the α_L I domain C-terminal linker totally abolished Mn^{2+} -induced ICAM-1 binding (Fig. 4). Mutation of another nearby acidic residue in the C-terminal linker of the α_L I domain, α_L -E310A, only partially reduced Mn^{2+} -induced ligand binding and served as a control (Fig. 4). Consistent with our previous conclusion that compound 4 binds to the MIDAS of the β_2 I domain (37), the β_2 Ser-114 mutation completely abolished both inhibition of ICAM-1 binding in Mn^{2+} by compound 4 and stimulation of ICAM-1 binding in $\text{Ca}^{2+}/\text{Mg}^{2+}$ by compound 4 (Fig. 4). Despite the absolute requirement for α_L -Glu-310 in Mn^{2+} -induced ICAM-1 binding by $\alpha_L\beta_2$, compound 4 was able to activate binding to ICAM-1 by the α_L -E310A mutant, demonstrating that compound 4 activates $\alpha_L\beta_2$ by a mechanism that is distinct from that of Mn^{2+} .

Susceptibility to $\alpha_L\beta_2$ Inhibitory Antibodies—mAbs exist that inhibit $\alpha_L\beta_2$ function by distinct mechanisms. Whereas some mAbs bind to the α_L I domain and competitively block ICAM-1 binding, other α_L I domain and β_2 I domain mAbs block ICAM-1 binding indirectly through allosteric mechanisms (34, 45, 46). We compared inhibition by a panel of these mAbs of CBR LFA-1/2-activated $\alpha_L\beta_2$ (wild type + mAb); α_L -Glu-310C/ β_2 -A210C (CC), an $\alpha_L\beta_2$ mutant that is constitutively activated by introducing an intersubunit disulfide bond between residue 210 in a β_2 I domain MIDAS loop and the α_L -Glu-310 residue (33); $\alpha_L\beta_2$ activated by compound 4 in $\text{Ca}^{2+}/\text{Mg}^{2+}$ (wild type + #4); and $\alpha_L\beta_2$ activated by a disulfide bond mutationally introduced into the α_L I domain (HA) (Table 1). The α_L -E310C/ β_2 -A210C mutant and

TABLE 1

Inhibition by α_L I and β_2 I domain antibodies of multimeric ICAM-1 binding to $\alpha_L\beta_2$ mutants

Wild-type (WT) $\alpha_L\beta_2$ in K562 transfectants was activated by preincubation with 10 $\mu\text{g}/\text{ml}$ mAb CBR LFA-1/2 (WT + mAb) or 1 μM compound 4 (WT + #4). CC, α_L -E310C/ β_2 -A210C. HA, $\alpha_L\beta_2$ with the high affinity K287C/K294C I domain mutation. Binding to soluble, multimeric ICAM-1 in medium containing 1 mM CaCl_2 and 1 mM MgCl_2 was in the presence of the indicated mAb. All mAbs bound to α_L -E310C/ β_2 -A210C, K287C/K294C, and wild-type $\alpha_L\beta_2$ with or without compound 4 equally well (data not shown).

mAb	Domain	Epitope	Inhibition			
			WT + mAb	CC	WT + #4	HA
				%		
TS2/6	α_L I	154–183	97	96	99	97
May.035	α_L I	Lys-197, His-201	98	98	99	97
MHM24	α_L I	Lys-197	96	97	98	96
TS1/22	α_L I	Gln-266, Ser-270	96	97	96	92
TS2/14	α_L I	Ser-270, Glu-272	99	99	99	14
May.017	β_2 I	Glu-175, ?	98	70	82	3
MHM23	β_2 I	Glu-175	97	40	12	2
TS1/18	β_2 I	Arg-133, His-332	98	4	0	0
YFC51	β_2 I	Arg-133, His-332	98	2	0	0
CLB LFA-1/1	β_2 I	His-332, Asn-339	97	2	0	0

wild-type $\alpha_L\beta_2$ activated by compound 4 showed almost identical susceptibility, *i.e.* they were inhibited by both the competitive α_L I domain mAbs and the allosteric TS2/14 α_L I domain mAb, were partially inhibited by mAb to Glu-175 in the specificity-determining loop of the β_2 I domain, and were resistant to mAbs to residues in the α 1 helix (133) and α 7 helix (332 and 339) of the β_2 I domain.

Effect of Compounds on $\alpha_L\beta_2$ Conformation—mAbs m24 and KIM127 represent reporters for $\alpha_L\beta_2$ active conformations. Whereas m24 recognizes the active conformation of the β_2 I domain, KIM127 binds to an epitope in the β_2 EGF2 domain that is buried in the bent (*i.e.* latent) integrin conformation and exposed in the extended (*i.e.* active) conformation. Compounds 3–5 induced exposure of the m24 and KIM127 epitopes on cell surface $\alpha_L\beta_2$ with similar dose responses (Fig. 5A and B), in agreement with previous measurements on purified $\alpha_L\beta_2$ with compounds 4 and 5 (37).

We previously developed a FRET method to monitor the spatial proximity of α_L and β_2 cytoplasmic domains in living cells by fusing mCFP and mYFP to the C termini of α_L and β_2 , respectively (43). Efficient FRET can only be observed when the cytoplasmic tails of α_L and β_2 (and, therefore, the fused mCFP and mYFP) are in close proximity. Consistent with our previous observations (43), we found here that stable K562 cell transfectants expressing α_L -mCFP/ β_2 -mYFP exhibited a significant FRET signal under basal conditions and that FRET was significantly decreased by treatment with Mn^{2+} plus soluble monomeric ICAM-1 (Fig. 5C). Exposure to either compound 4 or 5 in $\text{Ca}^{2+}/\text{Mg}^{2+}$ also statistically significantly reduced FRET, although to a somewhat lesser extent. These data suggest that compounds 4 and 5, consistent with induction of exposure of the m24 and KIM127 epitopes (Fig. 5, A and B), induce spatial separation of the α_L and β_2 cytoplasmic domains (Fig. 5C).

Compounds 4 and 5 Inhibit Lymphocyte Transendothelial Migration by Distinct Mechanisms—To assess the effects of compounds on transendothelial migration, *i.e.* diapedesis, we monitored migration of interleukin-2-cultured primary human lymphocytes through TNF- α -activated HUVEC monolayers in medium with $\text{Ca}^{2+}/\text{Mg}^{2+}$ by confocal microscopy. Under control conditions, efficient lymphocyte transendothelial migration was observed ($\sim 45\%$ by 10 min and $\sim 70\%$ by 60 min). Compared with control, compound 4, compound 5, and

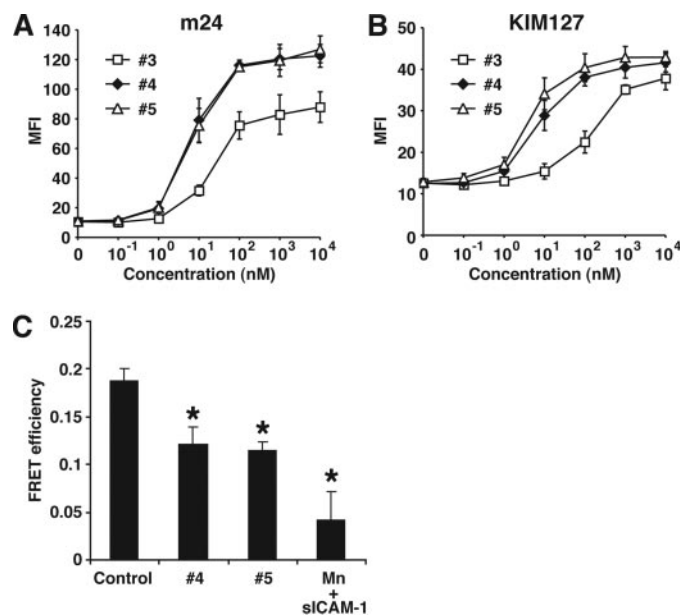


FIGURE 5. Effect of compounds on the conformation of $\alpha_L\beta_2$. A and B, effect of compounds on expression of activation epitopes on $\alpha_L\beta_2$. $\alpha_L\beta_2$ -Expressing K562 cells were stained with m24 (A) or KIM127 (B) in HEPES buffer containing 1 mM CaCl_2 , 1 mM MgCl_2 and compounds at 37 °C for 30 min followed by immunofluorescence flow cytometry. C, binding of compounds induces spatial separation of $\alpha_L\beta_2$ cytoplasmic domains. FRET was measured in α_L -mCFP/ β_2 -mYFP K562 transfectants after treatment with compounds (1 μM) or 1 mM Mn^{2+} and soluble monomeric ICAM-1 (sICAM-1) 100 $\mu\text{g}/\text{ml}$ as indicated. Data are the mean \pm S.E. for 8 to 10 cells. *, $p < 0.05$ versus control. MFI, mean fluorescence intensity.

BIRT377, an α I allosteric antagonist (Fig. 6A), all inhibited transendothelial migration by greater than 2-fold. Interestingly, Fab fragments of the $\alpha_L\beta_2$ -activating antibody, CBR LFA-1/2, also produced a comparable inhibition of diapedesis (Fig. 6A).

Despite similarity in overall extent of inhibition of diapedesis, morphological analysis (as described under “Experimental Procedures”) revealed dramatic differences among these antagonists (Fig. 6, B–D). Under control conditions (Me_2SO), the majority of the cells were polarized, whereas the remaining cells were equally divided into round and spread populations. In the presence of either compound 5 or BIRT377, the polarized cell population was reduced by greater than 2-fold, and the round cell population was dominant (Fig. 6, C and D). In stark contrast, for both compound 4 and CBR LFA-1/2 Fab treatments,

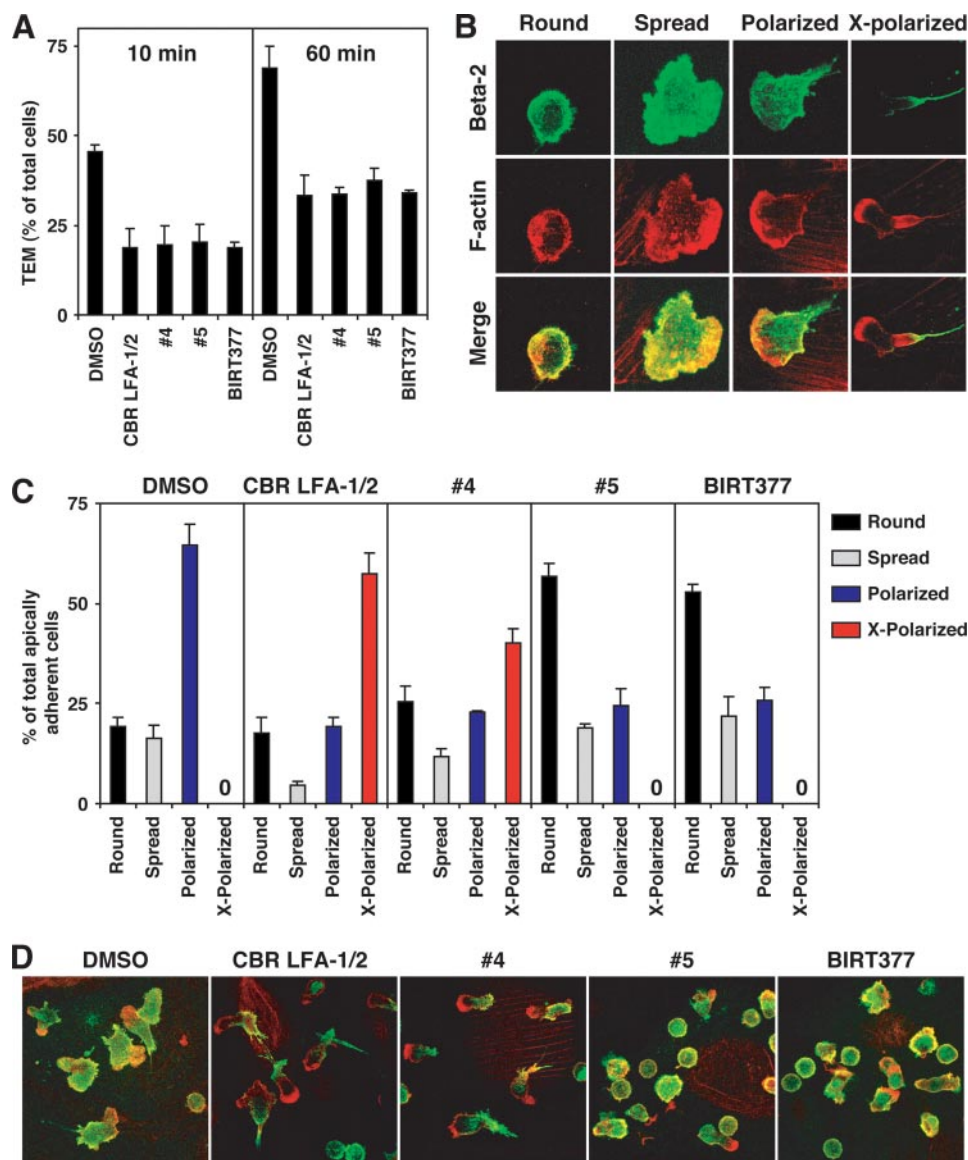


FIGURE 6. Effect of compounds on lymphocyte diapedesis. Interleukin-2-cultured human lymphocytes were incubated with TNF- α activated HUVEC monolayers for 10 or 60 min (A) or 10 min (B–D) in the absence or presence of compounds or CBR LFA-1/2 Fab, fixed, and stained as described under “Experimental Procedures.” For each experiment a minimum of 100 lymphocytes from randomly selected fields were carefully analyzed to determine stage of diapedesis and morphology as described under “Experimental Procedures.” A, quantitation of transendothelial migration (TEM). The number of cells having either initiated or completed diapedesis is expressed as a percentage of total cells. Values represent mean \pm S.E. of 3–6 independent experiments. DMSO, dimethyl sulfoxide. B–D, morphologic characterization of lymphocytes. Lymphocytes and HUVECs were fixed and stained for α_L integrin (green) and F-actin (red). Representative micrographs demonstrate each of four principal morphologic categories (round, spread, polarized, and X-polarized) observed among the apically adherent cells. C, the number of cells displaying each of the morphologies is expressed as a percentage of the total. Values represent mean \pm S.E. of 3–8 experiments. D, representative fields used for the quantitation shown in C.

the major cell population was in an unphysiologic “extremely polarized” (X-polarized) state in which the uropod was extended in length and dramatically enriched in $\alpha_L\beta_2$, concomitant with depletion of $\alpha_L\beta_2$ from other regions of the cell (Fig. 6, B–D).

The findings that compound 4 and CBR-LFA1/2 activate adhesiveness and induce extreme polarization and localization of LFA-1 to the uropod suggest that they may suppress lymphocyte migration by preventing de-adhesion of the uropod. To test the hypothesis that compound 4 inhibits migration, we per-

formed live-cell imaging of lymphocytes migrating on endothelial monolayers (Fig. 7 and supplemental Videos 1 and 2). Quantitative analysis of more than 50 lymphocytes revealed a greater than 2-fold reduction by compound 4 in both average lateral migration velocity and in the mean displacement of the lymphocytes and a nearly 3-fold reduction in the frequency of diapedesis (Fig. 7, A and B). Analysis of the live-cell imaging demonstrates that, in contrast to the relatively steady and smooth migration observed under control conditions (Fig. 7, C and E, and Video 1), compound 4 promotes “jerky” or “frustrated” migration in which the leading edge and cell body repeatedly advance, then become partially retracted back toward the uropod (Fig. 7, D–E, and Video 2).

DISCUSSION

The interaction between $\alpha_L\beta_2$ and ICAM-1 plays a critical role in the formation of the immunological synapse in immune responses and in leukocyte adhesion and extravasation through endothelium. $\alpha_L\beta_2$ is a clinically validated target for the treatment of autoimmune disease, and small molecule antagonists of $\alpha_L\beta_2$ are under intense investigation. Here, we show that a class of compounds previously classified as α/β I allosteric antagonists includes among its members a compound that is an agonist of $\alpha_L\beta_2$ in the presence of physiologic divalent cations, *i.e.* Ca^{2+} and Mg^{2+} . In contrast, compound 4 is an antagonist in Mn^{2+} , as previously reported (17, 37). Agonism in $\text{Ca}^{2+}/\text{Mg}^{2+}$ and antagonism in Mn^{2+} was consistently observed in soluble multimeric ICAM-1 binding assays, static cell adhesion, and flow chamber assays and with both K562 transfectants expressing $\alpha_L\beta_2$ and physiologic leukocytes, *i.e.* PBMCs. In parallel assays the structurally homologous compounds 3 and 5 (XVA143) exhibit only antagonistic properties. The finding that compound 4 can act as both an agonist and antagonist support our previous conclusion that it is an allosteric effector (37) and does not mimic and directly compete binding of ICAM-1 (17, 47).

Compounds 3–5 (XVA143) have very similar structures and appear to have overlapping binding sites. The ability of all three

Small Molecule Agonist of an Integrin, $\alpha_L\beta_2$

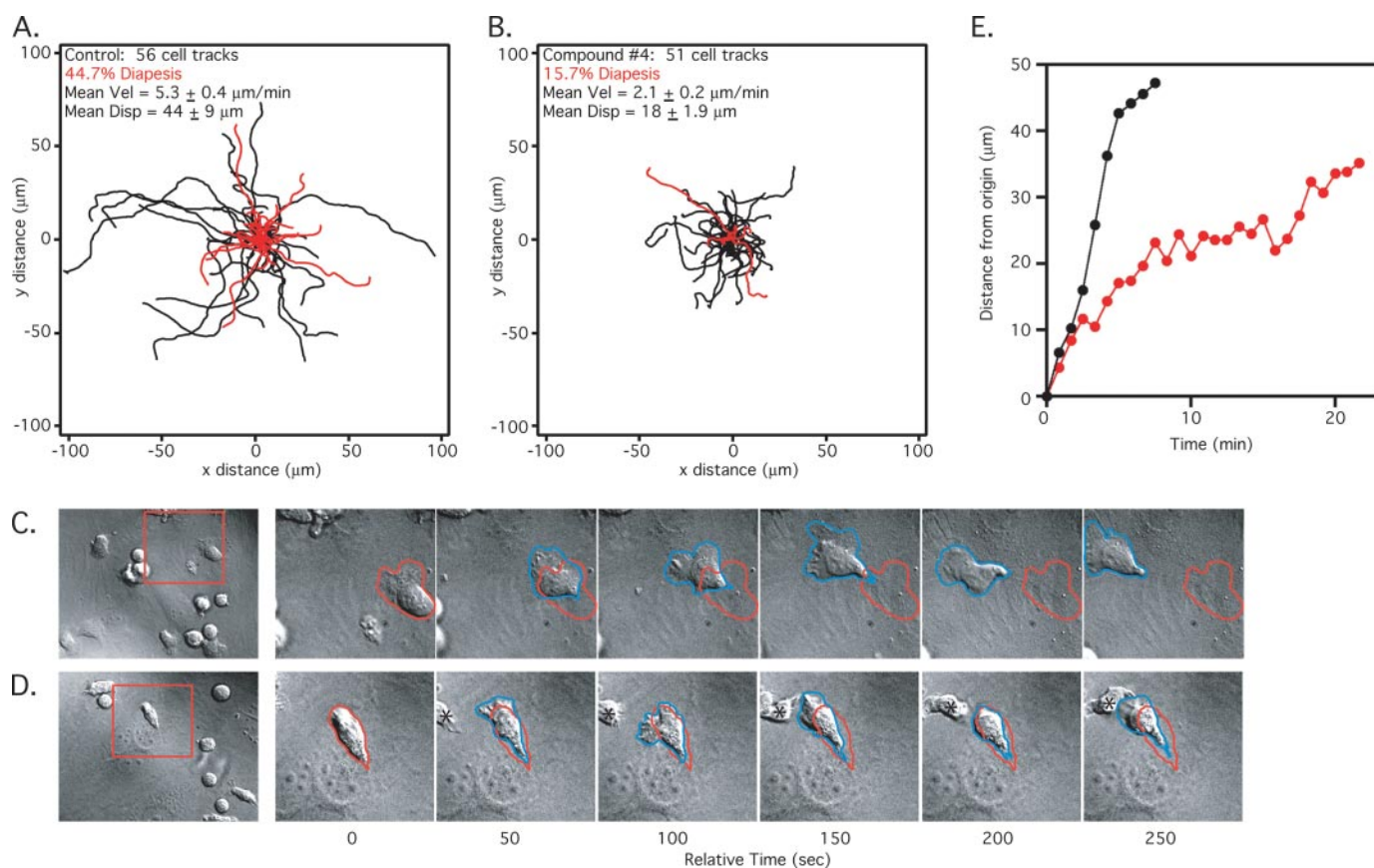


FIGURE 7. Dynamics of lymphocyte lateral migration and diapedesis across endothelium. Live-cell imaging and analysis of lymphocytes migrating on TNF- α -activated HUVEC monolayers was as described under "Experimental Procedures." For each condition, greater than 50 cells, taken from four separate imaging experiments (see representative experiments in supplemental Videos 1 and 2) were analyzed. *A* and *B*, two-dimensional tracks of lymphocytes migrating over a 30-min period under control conditions (*A*) and in the presence of $1 \mu\text{M}$ compound 4 (*B*). Tracks of cells that initiated diapedesis during the imaging time course are terminated at the point of initiation of diapedesis and are depicted in red. *C–E*, kinetics of migration of representative lymphocytes. *C–D*, left panels are selected frames from representative live-cell imaging experiments under control condition (*C*, see Video 1) and in the presence of compound 4 (*D*, see Video 2). Representative cells (boxed region in left panels) were tracked at 50-s intervals. The outline (red) of the cell position at relative time 0 is shown in all panels. Note that in control condition (*C*) the migrating cell steadily increases its distance from its origin over time, whereas in the presence of compound 4 (*D*) the cell repeatedly moves away from and then contracts back toward the origin. *E*, the distances from the origin of the centroids of the two migrating cells shown in *C* and *D* are plotted against time for control (black) and compound 4 (red) conditions. The control cell is only tracked for 7 min because after this it left the boxed region in Fig. 7C.

compounds to stabilize non-covalent association of the α_L and β_2 subunits in SDS-PAGE is not dependent on the α_L I domain and is absolutely dependent on divalent cations and the β_2 I domain MIDAS residue Ser-114. Mn^{2+} and $\text{Ca}^{2+}/\text{Mg}^{2+}$ each support stabilization of $\alpha_L\beta_2$ and $\alpha_M\beta_2$ noncovalent complexes in SDS-PAGE. All three compounds inhibit ligand binding by $\alpha_M\beta_2$ as well as $\alpha_L\beta_2$ (37). Antagonism and agonism by compound 4 appear to occur at the same binding site, since the closely related compound 5 competitively antagonizes agonism by compound 4, and agonism requires β_2 I domain residue Ser-114.

The mechanism of α_L I domain activation by compound 4 differs somewhat from mechanisms previously described for other α_L I domain activators. For $\alpha_L\beta_2$ stimulated with either Mn^{2+} or CBR LFA-1/2, mutation of Glu-310 to Ala at the C-terminal α_L I domain linker results in loss of ligand binding by abolishing the interdomain communication between the α I and β I domains (33). The lack of dependence on Glu-310 in compound 4-induced $\alpha_L\beta_2$ activation suggests that compound 4 makes distinct contacts with the α_L I domain or its linker that cause activation. However, at the same time, compound 4 (like

other α/β I allosteric antagonists) apparently blocks the Glu-310- β_2 MIDAS interaction through competition for the binding to the MIDAS (37). Wild-type $\alpha_L\beta_2$ activated by compound 4 showed almost identical susceptibility to inhibitory antibodies as α_L -E310C/ β_2 -A210C, which is consistent with the notion that compound 4 induces interaction between the β_2 I domain MIDAS and the C-terminal α_L I domain linker similarly to the engineered disulfide bond in α_L -E310C/ β_2 -A210C. The similarity between these activation mechanisms is further supported by our previous finding that α_L -E310C/ β_2 -A210C exhibits less binding to soluble multimeric ICAM-1 in Mn^{2+} than in $\text{Ca}^{2+}/\text{Mg}^{2+}$ (33).

Our working model for agonism by compound 4 is as follows. Ca^{2+} and Mn^{2+} compete for binding to the Adjacent to MIDAS (ADMIDAS) metal ion binding site and by binding to this site inhibit and stimulate ligand binding, respectively, and coordinate with alternative ADMIDAS residues (48). In both $\text{Ca}^{2+}/\text{Mg}^{2+}$ and Mn^{2+} , compounds 3–5 (XVA143) bind to the β_2 MIDAS and block its interaction with α_L -Glu-310. In $\text{Ca}^{2+}/\text{Mg}^{2+}$, the complex between compound 4 and the β_2 I domain is slightly altered compared with its conformation in Mn^{2+} so

that it is complementary to and can bind to the α_L I domain or its linker and induce the open conformation of the α_L I domain through interactions that do not involve, but functionally substitute for, the α_L -Glu-310: β_2 -MIDAS interaction.

Despite agonistic stimulation of ligand binding, compound 4 can still block physiologic functions of $\alpha_L\beta_2$ that require cycles of adhesion and detachment. It has been proposed that integrins are active at the leading edge, whereas they are inactive at the trailing edge of migrating leukocytes (49, 50). Inactivation of integrins at the trailing edge is thought to be important for detaching the uropod (51). Indeed, sustained activation of β_1 or β_2 via activating antibodies (52, 53) or blockade of Rho signaling (54) suppressed eosinophil and monocyte transmigration by preventing the trailing edge from being detached.

We found that although compounds 4 and 5, BIRT377, and CBR LFA-1/2 all inhibit lymphocyte transmigration across the endothelium cell layer, they do so by different mechanisms. Compound 5 and BIRT377 distinctly promoted a predominant round cell population, with greatly reduced spreading and polarization consistent with a reduction in overall adhesiveness. In contrast, compound 4 and CBR LFA-1/2 Fab induced the migrating lymphocytes to display unusually long uropods that were highly enriched in $\alpha_L\beta_2$, consistent with increased adhesion and decreased de-adhesion in the trailing edge. This was confirmed by live-cell imaging analysis that demonstrated frustrated lateral migration induced by compound 4, in which failure of the uropod to detach limited lymphocyte migration. Thus, compound 5 (XVA143) blocks transendothelial migration by reducing adhesion, whereas compound 4 and CBR LFA-1/2 Fab block transendothelial migration by activating $\alpha_L\beta_2$ and interfering with uropod detachment. In a related finding, mutant mice expressing constitutively active $\alpha_L\beta_2$ were impaired in T cell migration, T cell proliferation stimulated by antigen presenting cells, cytotoxic T cell activity, T-dependent humoral immune responses, and neutrophil recruitment during aseptic peritonitis, although signaling through $\alpha_L\beta_2$ was not affected (31). The above observations are consistent with the previous report that compound 4 is a potent inhibitor of the mixed lymphocyte reaction (17). Our study demonstrates for the first time a small molecule integrin allosteric agonist that functions as an anti-inflammatory drug through a novel mechanism of action, perturbation of integrin de-adhesion.

Compound 4 is the first small molecule agonist reported for any integrin. Integrin agonists open up novel opportunities for therapeutics that increase rather than decrease integrin-dependent adhesion. For example, immune recognition of tumor cells is LFA-1-dependent, and agonists might enhance immune responses, including cytotoxic killing of tumor cells. Although we have found that agonism of $\alpha_L\beta_2$ decreases cell migration, and mice with permanently up-regulated $\alpha_L\beta_2$ are functionally impaired, appropriate dosing could allow cycles of agonism at peak drug levels to be alternated with cell migration during intervening troughs. There is extensive precedent with G-protein-coupled receptors for closely related compounds to act as agonists and antagonists (inverse agonists), and both types of compounds have important therapeutic applications.

REFERENCES

- Anderson, D. C., Smith, C. W., and Springer, T. A. (1989) in *Metabolic Basis of Inherited Disease* (Stanbury, J. B., Wyngaarden, J. B., and Fredrickson, D. S., eds) 6th Ed., pp. 2751–2777, McGraw-Hill, New York
- Springer, T. A. (1990) *Nature* **346**, 425–433
- Harlan, J. M., Winn, R. K., Vedder, N. B., Doerschuk, C. M., and Rice, C. L. (1992) in *Adhesion: Its Role in Inflammatory Disease* (Harlan, J. R., and Liu, D., eds) pp. 117–150, W. H. Freeman and Co., New York
- Giblin, P. A., and Kelly, T. A. (2001) *Annu. Rep. Med. Chem.* **36**, 181–190
- Yusuf-Makagiansar, H., Anderson, M. E., Yakovleva, T. V., Murray, J. S., and Siahaan, T. J. (2002) *Med. Res. Rev.* **22**, 146–167
- Gottlieb, A. B., Krueger, J. G., Bright, R., Ling, M., Lebwohl, M., Kang, S., Feldman, S., Spellman, M., Wittkowski, K., Ochs, H. D., Jardieu, P., Bauer, R., White, M., Dedrick, R., and Garovoy, M. (2000) *J. Am. Acad. Dermatol.* **42**, 428–435
- Gottlieb, A. B., and Bos, J. D. (2002) *Clin. Immunol.* **105**, 105–116
- Gottlieb, A. B., Krueger, J. G., Wittkowski, K., Dedrick, R., Walicke, P. A., and Garovoy, M. (2002) *Arch. Dermatol.* **138**, 591–600
- Cather, J. C., and Menter, A. (2003) *Expert Opin. Biol. Ther.* **3**, 361–370
- Lebwohl, M., Tyring, S. K., Hamilton, T. K., Toth, D., Glazer, S., Tawfik, N. H., Walicke, P., Dummer, W., Wang, X., Garovoy, M. R., and Pariser, D. (2003) *N. Engl. J. Med.* **349**, 2004–2013
- Weitz-Schmidt, G., Welzenbach, K., Brinkmann, V., Kamata, T., Kallen, J., Bruns, C., Cottens, S., Takada, Y., and Hommel, U. (2001) *Nat. Med.* **7**, 687–692
- Kallen, J., Welzenbach, K., Ramage, P., Geyl, D., Kriwacki, R., Legge, G., Cottens, S., Weitz-Schmidt, G., and Hommel, U. (1999) *J. Mol. Biol.* **292**, 1–9
- Last-Barney, K., Davidson, W., Cardozo, M., Frye, L. L., Grygon, C. A., Hopkins, J. L., Jeanfavre, D. D., Pav, S., Qian, C., Stevenson, J. M., Tong, L., Zindell, R., and Kelly, T. A. (2001) *J. Am. Chem. Soc.* **123**, 5643–5650
- Liu, G., Huth, J. R., Olejniczak, E. T., Mendoza, R., DeVries, P., Leitza, S., Reilly, E. B., Okasinski, G. F., Fesik, S. W., and von Geldern, T. W. (2001) *J. Med. Chem.* **44**, 1202–1210
- Burdick, D. J. (March 24, 1999) International Patent WO9949856
- Burdick, D. J., Gadek, T. R., Marsters, J., Oare, D. A., Reynolds, M. E., and Stanley, M. S. (November 26, 2001) International Patent WO02059114
- Gadek, T. R., Burdick, D. J., McDowell, R. S., Stanley, M. S., Marsters, J. C., Jr., Paris, K. J., Oare, D. A., Reynolds, M. E., Ladner, C., Zioncheck, K. A., Lee, W. P., Gribling, P., Dennis, M. S., Skelton, N. J., Tumas, D. B., Clark, K. R., Keating, S. M., Beresini, M. H., Tilley, J. W., Presta, L. G., and Bodary, S. C. (2002) *Science* **295**, 1086–1089
- Humphries, M. J. (2000) *Biochem. Soc. Trans.* **28**, 311–339
- Gahmberg, C. G., Tolvanen, M., and Kotovuori, P. (1997) *Eur. J. Biochem.* **245**, 215–232
- Shimaoka, M., Takagi, J., and Springer, T. A. (2002) *Annu. Rev. Biophys. Biomol. Struct.* **31**, 485–516
- Lee, J.-O., Rieu, P., Arnaout, M. A., and Liddington, R. (1995) *Cell* **80**, 631–638
- Huang, C., Zang, Q., Takagi, J., and Springer, T. A. (2000) *J. Biol. Chem.* **275**, 21514–21524
- Xiong, J.-P., Stehle, T., Diefenbach, B., Zhang, R., Dunker, R., Scott, D. L., Joachimiak, A., Goodman, S. L., and Arnaout, M. A. (2001) *Science* **294**, 339–345
- Song, G., Yang, Y., Liu, J.-h., Casanovas, J., Shimaoka, M., Springer, T. A., and Wang, J.-h. (2005) *Proc. Natl. Acad. Sci. U. S. A.* **102**, 3366–3371
- Shimaoka, M., Shifman, J. M., Jing, H., Takagi, J., Mayo, S. L., and Springer, T. A. (2000) *Nat. Struct. Biol.* **7**, 674–678
- Shimaoka, M., Lu, C., Palframan, R., von Andrian, U. H., Takagi, J., and Springer, T. A. (2001) *Proc. Natl. Acad. Sci. U. S. A.* **98**, 6009–6014
- Takagi, J., Petre, B. M., Walz, T., and Springer, T. A. (2002) *Cell* **110**, 599–611
- Luo, B.-H., Takagi, J., and Springer, T. A. (2004) *J. Biol. Chem.* **279**, 10215–10221
- Yang, W., Shimaoka, M., Chen, J. F., and Springer, T. A. (2004) *Proc. Natl. Acad. Sci. U. S. A.* **101**, 2333–2338
- Xiao, T., Takagi, J., Wang, J.-h., Collier, B. S., and Springer, T. A. (2004)

Small Molecule Agonist of an Integrin, $\alpha_L\beta_2$

- Nature* **432**, 59–67
31. Semmrich, M., Smith, A., Feterowski, C., Beer, S., Engelhardt, B., Busch, D. H., Bartsch, B., Laschinger, M., Hogg, N., Pfeffer, K., and Holzmann, B. (2005) *J. Exp. Med.* **201**, 1987–1998
 32. Alonso, J. L., Essafi, M., Xiong, J. P., Stehle, T., and Arnaout, M. A. (2002) *Curr. Biol.* **12**, 340–342
 33. Yang, W., Shimaoka, M., Salas, A., Takagi, J., and Springer, T. A. (2004) *Proc. Natl. Acad. Sci. U. S. A.* **101**, 2906–2911
 34. Lu, C., Shimaoka, M., Zang, Q., Takagi, J., and Springer, T. A. (2001) *Proc. Natl. Acad. Sci. U. S. A.* **98**, 2393–2398
 35. Fotouhi, N., Gillespie, P., Guthrie, R., Pietranico-Cole, S., and Yun, W. (October 12, 1999) International Patent WO0021920
 36. Welzenbach, K., Hommel, U., and Weitz-Schmidt, G. (2002) *J. Biol. Chem.* **277**, 10590–10598
 37. Shimaoka, M., Salas, A., Yang, W., Weitz-Schmidt, G., and Springer, T. A. (2003) *Immunity* **19**, 391–402
 38. Dransfield, I., and Hogg, N. (1989) *EMBO J.* **8**, 3759–3765
 39. Robinson, M. K., Andrew, D., Rosen, H., Brown, D., Ortlepp, S., Stephens, P., and Butcher, E. C. (1992) *J. Immunol.* **148**, 1080–1085
 40. Lu, C., and Springer, T. A. (1997) *J. Immunol.* **159**, 268–278
 41. Carman, C. V., and Springer, T. A. (2004) *J. Cell Biol.* **167**, 377–388
 42. Salas, A., Shimaoka, M., Kogan, A. N., Harwood, C., von Andrian, U. H., and Springer, T. A. (2004) *Immunity* **20**, 393–406
 43. Kim, M., Carman, C. V., and Springer, T. A. (2003) *Science* **301**, 1720–1725
 44. Huth, J. R., Olejniczak, E. T., Mendoza, R., Liang, H., Harris, E. A., Lupher, M. L., Jr., Wilson, A. E., Fesik, S. W., and Staunton, D. E. (2000) *Proc. Natl. Acad. Sci. U. S. A.* **97**, 5231–5236
 45. Lu, C., Shimaoka, M., Ferzly, M., Oxvig, C., Takagi, J., and Springer, T. A. (2001) *Proc. Natl. Acad. Sci. U. S. A.* **98**, 2387–2392
 46. Lu, C., Shimaoka, M., Salas, A., and Springer, T. A. (2004) *J. Immunol.* **173**, 3972–3978
 47. Keating, S. M., Clark, K. R., Stefanich, L. D., Arellano, F., Edwards, C. P., Bodary, S. C., Spencer, S. A., Gadek, T. R., Marsters, J. C., Jr., and Beresini, M. H. (2006) *Protein Sci.* **15**, 290–303
 48. Chen, J. F., Salas, A., and Springer, T. A. (2003) *Nat. Struct. Biol.* **10**, 995–1001
 49. Springer, T. A., and Anderson, D. C. (1986) in *Biochemistry of Macrophages (Ciba Symposium 118)* pp. 102–126, Pitman, London
 50. Smith, A., Bracke, M., Leitinger, B., Porter, J. C., and Hogg, N. (2003) *J. Cell Sci.* **116**, 3123–3133
 51. Sanchez-Madrid, F., and del Pozo, M. A. (1999) *EMBO J.* **18**, 501–511
 52. Kuijpers, T. W., Mul, E. P. J., Blom, M., Kovach, N. L., Gaeta, F. C. A., Tollefson, V., Elices, M. J., and Harlan, J. M. (1993) *J. Exp. Med.* **178**, 279–284
 53. Weber, C., Lu, C.-F., Casasnovas, J. M., and Springer, T. A. (1997) *J. Immunol.* **159**, 3968–3975
 54. Worthylyake, R. A., Lemoine, S., Watson, J. M., and Burridge, K. (2001) *J. Cell Biol.* **154**, 147–160